Sensitivity analysis for photonic crystal microcavities

Zhen Hu[1,*] and Ya Yan Lu[2]

[1] Department of Mathematics, Hohai University, Nanjing, Jiangsu, China
[2] Department of Mathematics, City University of Hong Kong, Kowloon, Hong Kong
* Corresponding author: huzhen1230@gmail.com

Resonant modes in photonic crystal microcavities with large quality factors and small mode volumes are important in many applications, but they are very sensitive to geometric and physical parameters of the structure. In this paper, we develop an efficient method for computing the partial derivatives of the complex resonant frequency with respect to parameters such as radii, rafractive indices and positions of the circular cylinders, for two-dimensional photonic crystal microcavities. Like the adjoint variable method for sensitivity analysis, our method is capable of rapidly calculating the partial derivatives with respect to a large number of geometric and material parameters. The method is efficient, since it takes advantages of the many identical unit cells in photonic crystal devices and the analytic solutions for circular cylindrical structures.

1. INTRODUCTION

To understand the effect of fabrication errors and to find optimal designs for useful structures and devices, it is important to have efficient sensitivity analysis tools [1–7]. A necessary step of a sensitivity analsysis is to calculate the partial derivatives of a response function with respect to design parameters. For analyzing photonic devices, the mathematical problems can roughly be classified as boundary value problems and eigenvalue problems. For boundary value problems, a typical response function is the transmission coefficient of normalized power in an output channel. In that case, the objective is to calculate the partial derivatives of the transmission coefficient with respect to the design parameters. Eigenvalue problems are associated with non-trivial solutions without incident waves or sources. The "response function" should be replaced by the propagation constant of a waveguide mode, the wavevector of a Bloch mode in a peridic medium, or the frequency of a resonant mode in a cavity. It is clearly important to understand how these quantities vary with geometric or physical parameters of the device or structure.

Sensitivity analysis for photonic crystal (PhC) devices has been considered by a number of authors [4, 7, 8]. A particular important technique is the adjoint variable method which allows the rapid calculations of first order partial derivatives with respect to many design parameters using essentially only two field calculations. Since a typical PhC involves circular cylinders (dielectric rods or air-holes), it is particularly important to study the sensitivity with respect to the radii and locations of the circular cylinders. Notice that a typical PhC device has many identical unit cells, even though the periodicity may have been broken by intensionally introduced defects. In [7], we developed an efficient second order sensitivity analysis technique for idealized two-dimensional (2D) PhC devices, where the response function is the transmission coefficient in an output waveguide and the design parameters are the radii of the cylinders. This is related to a boundary value problem at a fixed frequency. The method is efficient, since it takes advantage of the many identical unit cells and the analytic solutions associated with circular cylinders.

In this paper, we develop an efficient method for sensitivity analysis of PhC microcavities in idealized 2D PhCs. The microcavities are allowed to couple to PhC waveguides, so that energy can leak out of the microcavity through the waveguides. A resonant mode in such a cavity is a non-trivial solution of the homogeneous Maxwell's equations satisfying proper outgoing radiation conditions, and it usually exists for a complex frequency. The real part of the complex frequency gives the normal resonant frequency and the imaginary part gives the damping rate of the mode. Based on the analytic solutions associated with circular cylinders and rigorous boundary conditions for terminating the PhC waveguides, we develop an efficient

method for computing the partial derivatives of the complex frequency with respect to the radii, refractive indices, and center positions of the cylinders. Like the standard adjoint variable method [3–5, 7], the partial derivatives with respect to the design parameters in many different unit cells can be efficiently calculated. To simplify the presentation, we concentrate on a 2D PhC with a square array of dielectric rods, and analyze a microcavity coupled to PhC waveguides.

2. WAVEGUIDE-CAVITY SYSTEM

As a simple example for illustrating our method, we consider the waveguide-cavity system shown in Fig. 1. The background
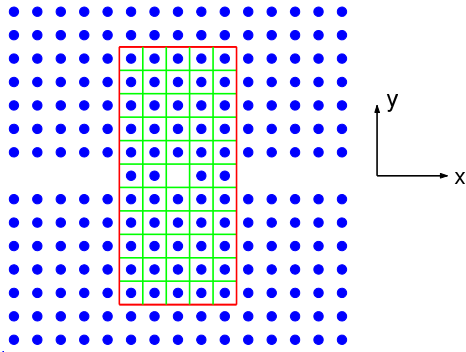
Fig. 1. A 2D photonic crystal waveguide-cavity system and the computational domain $\mathcal{D}$ with 11×5 square unit cells.

PhC is a square array of parallel and infinitely long dielectric rods surrounded by air, where the lattice constant is L, the radius and dielectric constant of the rods are $a = 0.2L$ and $\varepsilon = 11.4$, respectively. A PhC microcavity is formed by removing one single rod, and it is coupled to two semi-infinite PhC waveguides along the x axis. The waveguides are formed by removing a row of dielectric rods. In the horizontal direction, the missing rod at the center of the microcavity is surrounded by K regular rods in each side. The case of $K = 2$ is shown Fig. 1.

For the E polarization, the z component of the electric field, denoted by u in this paper, satisfies the following Helmholtz equation

$$\partial_x^2 u + \partial_y^2 u + k_0^2 n^2(\mathbf{r})u = 0, \tag{1}$$

where $\mathbf{r} = (x, y)$, $n(\mathbf{r})$ is the refractive index function, $k_0 = \omega/c$ is the free space wavenumber, ω is the angular frequency, c is the speed of light in vacuum. The assumed time dependence is $e^{-i\omega t}$ where i is the imaginary unit.

It is known that the PhC waveguide has a single propagating Bloch mode for $0.305 < \omega L/(2\pi c) < 0.422$. In this frequency range, we may specify an incoming propagating mode as the incident wave in the left waveguide. That is,

$$u^{(i)}(\mathbf{r}) = \psi_1(\mathbf{r})e^{i\beta_1 x},$$

where ψ_1 is periodic in x with period L and decays to zero as $y \to \pm\infty$, and β_1 is the real propagation constant (or Bloch wavenumber) of the mode. The transmitted wave in the right semi-infinite PhC waveguide can be expanded as

$$u^{(t)}(\mathbf{r}) = \sum_{j=1}^{\infty} C_j \psi_j(\mathbf{r})e^{i\beta_j x}, \tag{2}$$

where C_j is the coefficient of the jth Bloch mode of the PhC waveguide. Since the waveguide has only one propagating

mode, all other modes are evanescent. Therefore, $\text{Im}(\beta_j) > 0$ for $j > 1$, and the transmission coefficient (for normalized power) is simply

$$T = |C_1|^2. \tag{3}$$

Mathematically, the above is a boundary value problem of Eq. (1).

Without the incident wave, Eq. (1) with outgoing radiation conditions in both left and right waveguides, usually has only the zero solution for a given real frequency. A resonant mode is non-trivial solution of Eq. (1) which typically exists for a complex ω. The imaginary part of ω is negative, since it must decay with time under the assumed time dependence $e^{-i\omega t}$. The quality factor of the resonant mode is given by $Q = -2\text{Re}(\omega)/\text{Im}(\omega)$. Computing the resonant mode is an eigenvalue problem, where ω (or ω^2 or k_0^2) is the eigenvalue. However, it is an improper eigenvalue problem, since the wave field of a resonant mode (with a complex ω) blows up as $x \to \pm\infty$.

3. DTN-MAP METHOD

To analyze general 2D PhC devices, the Dirichlet-to-Neumann (DtN) map method may be used [10]. For the waveguide-cavity system shown in Fig. 1, the DtN-map method performs the computation in a domain $\mathcal{D}$ shown as the rectangle with red boundary in the figure. In addition, the method avoids the interiors of the square unit cells in $\mathcal{D}$, and formulates a small linear system for u on the edges of the unit cells only. The main steps of the DtN-map method are summarized below.

1. Choose an integer M and truncate the domain to $5M$ unit cells as shown in Fig. 1 (for the case of $M = 11$). Denote the truncated domain by $\mathcal{D}$, and assume it is given by $x_0 < x < x_5$ and $y_0 < y < y_M$, where $x_i = x_0 + iL$ and $y_j = y_0 + jL$.

2. For each unit cell Ω_k, calculate its DtN map $\mathbf{\Lambda}_k$, such that

$$\partial_\nu u = \mathbf{\Lambda}_k u \quad \text{on} \quad \partial\Omega_k, \tag{4}$$

where $\partial\Omega_k$ is the boundary of Ω_k, ∂_ν is ∂_x or ∂_y on the vertical or horizontal edges, respectively. If N points are used to discretize each edge of the unit cell, $\mathbf{\Lambda}_k$ is approximated by a $(4N) \times (4N)$ matrix.

3. Calculate operators $\mathbf{L}^+$ and $\mathbf{L}^-$ (approximated by $(NM) \times (NM)$ matrices) and a vector $\mathbf{g}$ related to the incident wave, such that the boundary conditions at x_0 and x_5 are

$$\partial_x u = \mathbf{L}^+ u, \qquad x = x_5, \tag{5}$$
$$\partial_x u = \mathbf{L}^- u + \mathbf{g}, \qquad x = x_0. \tag{6}$$

4. Formulate and solve a linear system

$$\mathbf{A}\mathbf{u} = \mathbf{f}, \tag{7}$$

where $\mathbf{u}$ is a column vector for u on all vertical edges at x_0, x_1, ..., x_5 and all horizontal edges at y_1, y_2, ..., y_{M-1}, and $\mathbf{f}$ is a vector related to the incident wave.

5. Find a vector $\mathbf{d}$ and then

$$C_1 = \mathbf{d}^T \mathbf{u}. \tag{8}$$

In the first step, the integer M is chosen so that $u \approx 0$ at the top and bottom boundaries of the truncated domain $\mathcal{D}$. The structure has only two distinct unit cells: the one with a rod and the one without. Therefore, it is only necessary to calculate two DtN maps. For simple unit cells, the DtN maps can be constructed from analytic solutions, i.e., the cylindrical waves [11, 12]. Equation (5) is a rigorous nonlocal boundary condition derived from the Bloch mode expansion (2). Equation (6) is inhomogeneous, since there is an incident wave in the left semi-infinite waveguide. Equation (7) is obtained by comparing $\partial_x u$ or $\partial_y u$ on the edges of the unit cells in $\mathcal{D}$. When u on the right boundary of $\mathcal{D}$ is known, the expansion coefficients in Eq. (2) can be calculated. This leads to Eq. (8), where d is a vector with NM non-zero entries.

The DtN-map method can also be used to find resonant modes [13]. In that case, there is no incident wave, thus g in Eq. (6) and f in Eq. (7) vanish. Notice that Λ_k, $L^{\pm}$ and A all depend on ω. The unknown ω can be solved iteratively from a condition that A is a singular matrix. We use the condition

$$\lambda_1(A) = 0, \tag{9}$$

where λ_1 is the eigenvalue of A with the smallest magnitude. In each iteration, we go through the second and third steps above (with $g = 0$), formulate the matrix A and find its eigenvalue λ_1. When ω is determined, the linear system (7) (with $f = 0$) has a nonzero solution u, then field distributions of the resonant mode can be constructed. More details can be found in [13].

4. SENSITIVITY OF TRANSMISSION COEFFICIENTS

In a previous work [7], we developed an efficient method for calculating the first and second order partial derivatives of the transmission coefficient T with respect to the radii of the rods. With a simple modification, the method can be used to compute the partial derivatives of T with respect to the refractive indices and the center positions of the rods. In the following, we explain the difference and present some numerical results.

Let Ω_i be a unit cell in the truncated domain $\mathcal{D}$ with a rod of radius a_i located at it center, and Λ_i be the DtN-map of Ω_i. As shown in [7], using the first and second order derivatives of the DtN-maps, we can evaluate the partial derivatives of A and C_1, then obtain $\partial T / \partial a_i$ and $\partial^2 T / \partial a_i \partial a_j$, where a_j is the radius of the rod in unit cell Ω_j. To analyze the sensitivity with respect to the positions of the rods, we assume the center of the rod in Ω_i moves from c_i to $c_i + p_i v_i$, where v_i is a unit vector and p_i is the distance, and attempt to calculate $\partial T / \partial p_i$ and $\partial^2 T / \partial p_i \partial p_j$ (at $p_i = 0$ and $p_j = 0$), where p_j and v_j are associated with unit cell Ω_j. These are actually directional derivatives with respect to the centers of the rods and the related unit vectors. We use the simple notations $\partial T / \partial p_i$ and $\partial^2 T / \partial p_i \partial p_j$, assuming the unit vectors are fixed.

To calculate the derivatives of Λ_i with respect to p_i, we notice that $\Lambda_i = ND^{-1}$, where D and N are $(4N) \times (4N)$ matrices, their entries depend on p_i and are known analytically. The entries of these two matrices and their partial derivatives with respect to p_i are given in Appendix A. The derivatives of Λ_i can be evaluated by the following formulas:

$$\frac{\partial \Lambda_i}{\partial p_i} = \left(\frac{\partial N}{\partial p_i} - \Lambda_i \frac{\partial D}{\partial p_i} \right) D^{-1}, \tag{10}$$

$$\frac{\partial^2 \Lambda_i}{\partial p_i^2} = \left(\frac{\partial^2 N}{\partial p_i^2} - \Lambda_i \frac{\partial^2 D}{\partial p_i^2} - 2 \frac{\partial \Lambda_i}{\partial p_i} \frac{\partial D}{\partial p_i} \right) D^{-1}. \tag{11}$$

To find the partial derivatives of T, we can follow the procedure given in [7] with ∂a_i and ∂a_j replaced by ∂p_i and ∂p_j, respectively. Similarly, if the refractive index of the rod in unit cell Ω_i is n_{1i}, we first calculate the 1st and 2nd order partial derivatives of D and N with respect to n_{1i}, then evaluate $\partial \Lambda_i / \partial n_{1i}$ and $\partial^2 \Lambda_i / \partial n_{1i}^2$, and finally obtain the partial derivatives of T. More details on given in Appendix B.

For a numerical example, we consider the waveguide-cavity system of Section 2 for normalized frequency $\omega L / (2\pi c) = 0.3795$. Since the transmission coefficient T is most sensitive to the rods near the center of the cavity, we consider the six marked rods shown in Fig. 2. The calculated derivatives are
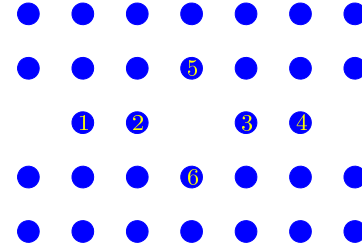
Fig. 2. The waveguide-cavity system of Fig. 1 with six rods near the center marked by integers 1, 2, ..., 6.

listed in Table 1, where the first and second order derivatives

Rod no. i	v_i	$L\,\partial_{p_i} T$	$L^2\,\partial_{p_i}^2 T$
1	(1,0)	2.856	37.4
2	(1,0)	33.340	5637.8
3	(1,0)	-33.340	5637.8
4	(1,0)	-2.856	37.4
5	(0,1)	-33.082	5593.3
6	(0,1)	33.082	5593.3

Table 1. Partial derivatives of the transmission coefficient T with respect to the moving distances of six marked rods in horizontal or vertical directions at $\omega L / (2\pi c) = 0.3795$.

are multiplied by L and L^2, respectively. The first four rods are located along the waveguide axis, and their horizontal derivatives are given in Table 1. It is clear that T is much more sensitive to the two rods (2 and 3) near the center of the cavity. Although the structure has a horizontal reflection symmetry, the wave field does not have the same symmetry, since it is excited by an incident propagating mode in the left semi-infinite waveguide. However, to the first a few digits shown in Table 1, the horizontal derivatives for each pair (rods 1 and 4, or rods 2 and 3) are identical or have opposite sign. This is a consequence of the Lorentz reciprocity theorem. The first order vertical derivatives of these four rods are identically zero, since both the structure and the wave field have a vertical reflection symmetry with respect to the waveguide axis. Their second order vertical derivatives are non-zero. For rod 2, the second order vertical derivative is $\partial_{p_2}^2 T = -58.1 L^{-2}$. For rods 5 and 6, we show the vertical derivatives in Table 1. Their values reflect the vertical reflection symmetry. We have also calculated the horizontal derivatives of these two rods. Their first order horizontal

derivatives are zero, again due to the reciprocity. Their second order horizontal derivatives are $-53.9L^{-2}$.

Of course, the partial derivatives can be calculated for any given direction. For rod 2 and $v_2 = (\sqrt{2}/2, \sqrt{2}/2)$, we obtain $\partial_{p_2} T = 23.591L^{-1}$ and $\partial_{p_2}^2 T = 2786.5L^{-2}$. Based on these derivatives, we can estimate the transmission coefficient T when the rods are moved by a small distance. In Table 2,

p_2/L	Taylor I	Taylor II	Exact value
0.002	0.3116	0.3171	0.3176
0.005	0.3824	0.4173	0.4256
0.008	0.4533	0.5425	0.5764
0.010	0.5005	0.6400	0.7003

Table 2. Exact and approximate transmission coefficients of the waveguide-cavity system at $\omega L/(2\pi c) = 0.3795$, when rod 2 is moved in the direction of $v_2 = (\sqrt{2}/2, \sqrt{2}/2)$.

we compare the approximate values of T obtained by truncated Taylor series with the exact value when rod 2 is moved by a small distance along the direction of v_2 given above. Considering T as a function of p_2, Taylor I and Taylor II in Table 2 are the Taylor series truncated to the first and second order derivatives, respectively. We observe that the exact T has large changes when the center of rod 2 is moved slightly, and the Taylor approximations are not very accurate. This is related to the resonant nature of this waveguide-cavity system. To accurately predict the shift of the transmission peaks or dips in a PhC device, we need to calculate the derivatives of the resonant frequencies with respect to design parameters.

5. SENSITIVITY OF RESONANT FREQUENCIES

The complex frequency ω of a resonant mode can be determined from the condition that A is a singular matrix [13]. For such a frequency, there is a nonzero solution u such that

$$Au = 0. \tag{12}$$

There is also a nonzero row vector h^T such that

$$h^T A = 0. \tag{13}$$

Let a_i be the radius of the rod in unit cell Ω_i, to find the partial derivative of ω with respect to a_i, we take the derivative for Eq. (12) and obtain

$$\frac{\partial A}{\partial \omega}\frac{\partial \omega}{\partial a_i}u + \frac{\partial A}{\partial a_i}u = -A\frac{\partial u}{\partial a_i}. \tag{14}$$

Multiplying h^T to both sides of Eq. (14), we have

$$\frac{\partial \omega}{\partial a_i} = -\frac{h^T \frac{\partial A}{\partial a_i} u}{h^T \frac{\partial A}{\partial \omega} u}. \tag{15}$$

Since we know how to evaluate $\partial A/\partial a_i$ [7], we concentrate on $\partial A/\partial \omega$ in the following.

The matrix A is constructed from the DtN maps of the unit cells in $\mathcal{D}$ and the boundary operators $L^{\pm}$. To find $\partial A/\partial \omega$, we need to evaluate $\partial \Lambda_i/\partial \omega$ and $\partial L^{\pm}/\partial \omega$. Since $\Lambda_i = ND^{-1}$, we have a formula similar to Eq. (10). The entries of D and N are given explicitly, thus their partial derivatives with respect to ω can be directly evaluated. The details are given in Appendix B.

To find $\partial L^{\pm}/\partial \omega$, we need to recall the procedure for constructing the boundary operator $L^{\pm}$. The details are given in [10]. The following steps are involved.

1. Truncate one period of the waveguide given by $x_{l-1} < x < x_l$ where $l \leq 0$ or $l > 2K+1$, to a supercell consisiting of M square unit cells with y given by $y_0 < y < y_M$.

2. Find a $(2MN) \times (2MN)$ matrix M, such that

$$M\begin{bmatrix} u_{l-1} \\ u_l \end{bmatrix} = \begin{bmatrix} M_{11} & M_{12} \\ M_{21} & M_{22} \end{bmatrix}\begin{bmatrix} u_{l-1} \\ u_l \end{bmatrix} = \begin{bmatrix} \partial_x u_{l-1} \\ \partial_x u_l \end{bmatrix}, \tag{16}$$

where u_l and $\partial_x u_l$ are column vectors of length NM for u and $\partial_x u$ at $x = x_l$, etc. M is also written in 2×2 blocks where each block is an $(MN) \times (MN)$ matrix.

3. Calculate the Bloch modes, $\psi_j(x,y)e^{\pm i\beta_j x}$, of the PhC waveguide by solving the matrix eigenvalue problem

$$\begin{bmatrix} M_{11} & -I \\ M_{21} & 0 \end{bmatrix}\begin{bmatrix} \psi_j \\ \partial_x \psi_j \end{bmatrix} = \mu_j \begin{bmatrix} -M_{12} & 0 \\ -M_{22} & I \end{bmatrix}\begin{bmatrix} \psi_j \\ \partial_x \psi_j \end{bmatrix}, \tag{17}$$

where $\mu_j = e^{i\beta_j L}$, ψ_j and $\partial_x \psi_j$ are vectors for ψ_j and $\partial_x \psi_j$ at $x = x_{l-1}$.

4. Define an $(MN) \times (MN)$ matrix T such that

$$T\psi_j = \mu_j \psi_j, \quad j = 1, 2, ..., MN. \tag{18}$$

The above can be written as

$$T\Psi = \Psi B, \tag{19}$$

where Ψ is the matrix with columns ψ_j and B is a diagonal matrix with diagonal entries μ_j for $1 \leq j \leq MN$.

5. The boundary operators $L^{\pm}$ are given by

$$L^+ = M_{11} + M_{12}T, \tag{20}$$
$$L^- = M_{21}T + M_{22}. \tag{21}$$

The matrix M is the DtN map of the supercell of the PhC waveguide. In [14], the eigenvalue problem, Eq. (17), was first formulated to solve the Bloch modes of PhC waveguides. The matrix M is constructed from the DtN maps of the unit cells assuming the boundary condition $u = 0$ at $y = y_0$ and $y = y_M$. Since we know how to evaluate the partial derivative with respect to ω of the DtN maps of the unit cells, $\partial M/\partial \omega$ can be easily evaluated.

To find the derivatives of ψ_j and μ_j with respect to ω, we rewrite Eq. (17) as

$$Ux_j = \mu_j V x_j \tag{22}$$

where U and V are the $(2MN) \times (2MN)$ matrices in the left and right hand sides of Eq. (17), and x_j denotes the column vector for ψ_j and $\partial_x \psi_j$. The derivative of Eq. (22) gives

$$\left(U - \mu_j V\right)\frac{\partial x_j}{\partial \omega} = \left(-\frac{\partial U}{\partial \omega} + \mu_j \frac{\partial V}{\partial \omega}\right)x_j + \frac{\partial \mu_j}{\partial \omega}Vx_j. \tag{23}$$

Let y_j be the right eigenvector satisfying $y_j^T(U - \mu_j V) = 0$, multiplying Eq. (23) by y_j^T, we obtain

$$\frac{\partial \mu_j}{\partial \omega} = \frac{y_j^T\left(\frac{\partial U}{\partial \omega} - \mu_j \frac{\partial V}{\partial \omega}\right)x_j}{y_j^T V x_j}. \tag{24}$$

Once $\partial\mu_j/\partial\omega$ is calculated, we can solve $\partial x_j/\partial\omega$ from Eq. (23). Since $U - \mu_j V$ is a singular matrix, we need to use the method of QR decomposition [15]. Notice that Eq. (23) is in general solvable, since its right hand side, denoted by z satisfies $y_j^\mathsf{T} z = 0$.

The remaining steps are straightforward. Taking the partial derivatives with respect to ω for Eqs. (19), (20) and (21), we obtain

$$\frac{\partial T}{\partial \omega} = \left[\frac{\partial \Psi}{\partial \omega} B + \Psi \frac{\partial B}{\partial \omega} - T \frac{\partial \Psi}{\partial \omega} \right] \Psi^{-1}, \qquad (25)$$

$$\frac{\partial L^+}{\partial \omega} = \frac{\partial M_{11}}{\partial \omega} + \frac{\partial M_{12}}{\partial \omega} T + M_{12} \frac{\partial T}{\partial \omega}, \qquad (26)$$

$$\frac{\partial L^-}{\partial \omega} = \frac{\partial M_{21}}{\partial \omega} T + M_{21} \frac{\partial T}{\partial \omega} + \frac{\partial M_{11}}{\partial \omega}. \qquad (27)$$

Therefore, once the partial derivatives of ψ_j and μ_j, $1 \le j \le MN$, are obtained, $\partial L^\pm/\partial\omega$ can be easily evaluated.

The sensitivity with respect to the refractive indices and the positions of the rods can be similarly studied. If the center of the rod in unit cell Ω_i moves from c_i to $c_i + p_i v_i$ for a fixed unit vector v_i and a variable distance p_i, $\partial\omega/\partial p_i$ at $p_i = 0$ can be evaluated by the formula

$$\frac{\partial \omega}{\partial p_i} = - \frac{h^\mathsf{T} \frac{\partial A}{\partial p_i} u}{h^\mathsf{T} \frac{\partial A}{\partial \omega} u}. \qquad (28)$$

Notice that $\partial A/\partial p_i$ and $\partial A/\partial\omega$ appear in the formula, and they can be evaluated by the methods discussed in Section 4 and in this section, respectively.

Similar to the standard adjoint variable method for sensitivity analysis [3–5, 7], our method is efficient for computing a large number of partial derivatives. From Eqs. (15) and (28), it is clear that we only need to calculate u, h^T and $\partial A/\partial\omega$ once. For $\partial A/\partial a_i$, $\partial A/\partial n_{1i}$ and $\partial A/\partial p_i$, we notice that these are very sparse matrices. As we mentioned earlier, A is constructed by matching the normal derivative of u on the edges of the unit cells, and it is related to the DtN maps of the unit cells and the boundary operators $L^\pm$. Since $\partial L^\pm/\partial a_i = 0$ and $\partial\Lambda_j/\partial a_i = 0$ if $i \ne j$, $\partial A/\partial a_i$ is only nonzero in a few blocks where Λ_i appears in A. The same is true for $\partial A/\partial n_{1i}$ and $\partial A/\partial p_i$. Since a unit cell is connected to four neighboring unit cells, Λ_i only appears in $4N$ rows of matrix A, where N is the number of points for discretizing one edge of the square unit cells. Furthermore, the DtN maps and their derivatives are identical for identical unit cells in different locations. Therefore, we only need to calculate the partial derivatives of the DtN maps for distinct unit cells.

6. NUMERICAL EXAMPLES

In this section, we consider the waveguide-cavity system similar to the one shown in Fig. 1, but for $K = 3$, where K is the number of regular rods in each side of the cavity center (a missing rod) along the waveguide axis. All other parameters are identical to those given in Section 2. In particular, all rods stay on lattice points of a square lattice, have a fixed dielectric constant $\varepsilon = 11.4$ and a constant radius $a = 0.2L$, where L is the lattice constant. A small part of the structure near the center of the cavity is shown in Fig. 3, where eight rods are marked by integers 1, 2, ..., 8.

In Fig. 4, we show the transmission spectrum of the structure (the blue curve with the peak in the middle), where the incident wave is a propagating mode of the PhC waveguide. The structure supports a resonant mode with a complex normalized frequency $\omega L/(2\pi c) = 0.3788761 - 0.0000417i$. The
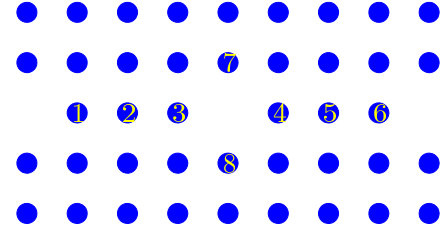
Fig. 3. A photonic crystal waveguide-cavity system with $K = 3$ rods on each side of the cavity center (a missing rod), and with eight rods marked by integers 1, 2, ..., 8.
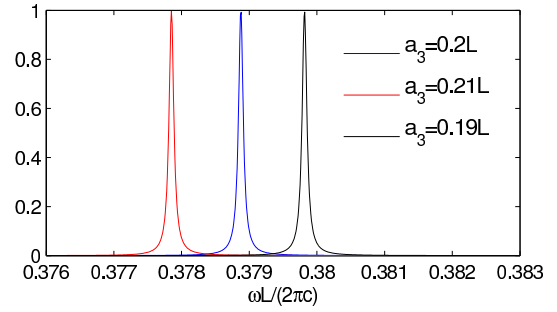
Fig. 4. Transmission spectra of the waveguide-cavity system shown in Fig. 3 (blue curve) and perturbed systems where the radius of rod 3 is changed to $0.21L$ (red curve) or $0.19L$ (black curve).

transmission property of the structure is very sensitive to the radii of rods near the center. In Fig. 4, the red and black curves are the transmission spectra when the radius of rod no. 3 is changed to $a_3 = 0.21L$ and $a_3 = 0.19L$, respectively. For these two values of a_3, the complex frequencies of the resonant modes are $\omega L/(2\pi c) = 0.3778499 - 0.0000419i$ and $\omega L/(2\pi c) = 0.3798165 - 0.0000423i$, respectively. The transmission spectra shown in Fig. 4 and the complex resonant frequencies are calculated by the DtN-map method developed in [10, 13] and summaried in Section 3.

The method described in the previous section is used to calculate the partial derivatives of the complex resonant frequency with respect to the radii of the rods. Let a_i for $i = 1, 2, ..., 8$, be the radii of the eight marked rods shown in Fig. 3, we list $\partial\omega/\partial a_i$ (at $a_i = 0.2L$) for rods $i = 1, 2, 3$ and 7 in Table 3. The re-

Rod no. i	$L^2/(2\pi c)\, \partial\omega/\partial a_i$
1	-0.0007563-0.0001867i
2	-0.0074756-0.0001540i
3	-0.0971303+0.0000192i
7	-0.0971130+0.0000847i

Table 3. Partial derivatives of the complex resonant frequency ω with respect to the radii of selected rods as shown in Fig. 3.

sults are given for the dimensionless quantity $L^2/(2\pi c)\partial\omega/\partial a_i$. The resonant mode has reflection symmetries in both horizontal and vertical directions, thus the partial derivatives with respect to a_4, a_5, a_6 and a_8 are identical to those with respect to a_3, a_2, a_1 and a_7. Notice that the real parts of $\partial\omega/\partial a_i$ are all negative, thus re-

increasing the radius of a rod will move the transmission peak to a lower frequency, consistent with the results shown in Fig. 4. The magnitudes of $\mathrm{Re}(\partial\omega/\partial a_i)$ comfirm that the resonant frequency is most sensitive to the rods closest to the center.

Using the partial derivatives, we can estimate the resonant frequency when the radii of the rods are changed slightly. In Table 4, we compare the exact and approximate values of the com-

$(a_3 - a)/L$	Taylor I	Exact value
0.002	0.3786819-0.0000417i	0.3786800-0.0000417i
0.004	0.3784876-0.0000416i	0.3784801-0.0000417i
0.006	0.3782934-0.0000416i	0.3782754-0.0000417i
0.008	0.3780991-0.0000416i	0.3780656-0.0000418i
0.010	0.3779048-0.0000415i	0.3778499-0.0000419i
-0.002	0.3790704-0.0000418i	0.3790688-0.0000418i
-0.004	0.3792647-0.0000418i	0.3792586-0.0000418i
-0.006	0.3794589-0.0000418i	0.3794462-0.0000420i
-0.008	0.3796532-0.0000419i	0.3796320-0.0000421i
-0.010	0.3798475-0.0000419i	0.3798165-0.0000423i

Table 4. Excat and approximates values of the normalized resonant frequency, $\omega L/(2\pi c)$, for a few values of a_3.

plex resonant frequency for a few different values of a_3, where the approximate values (denoted as Taylor I) are obtained by a Taylor series truncated to the first order derivative. We can see that the approximation is quite accurate.

The partial derivatives of the resonant frequency with respect to the refractive indices of the rods can also be easily calculated. In Table 5, we list the results for four rods shown in

Rod no. i	$L/(2\pi c)\,\partial\omega/\partial n_{1i}$
1	-0.0000511+0.0000068i
2	-0.0005485+0.0000054i
3	-0.0082147+0.0000215i
7	-0.0082206+0.0000015i

Table 5. Partial derivatives of the complex resonant frequency ω with respect to the refractive indices of selected rods as shown in Fig. 3.

Fig. 3. For the same reason, the results for rods 4, 5, 6 and 8 are identical to those for rods 3, 2, 1 and 7. Based on the first order partial derivatives, we can estimate the resonant frequencies when the refractive indices of the rods are slightly changed. In Table 6, we compare the exact and approximate resonant frequencies when the refractive index $n_{1,3}$ of the 3rd rod differs sligthly from its original value $n_1 = \sqrt{11.4}$.

We also analyze the sensitivity of the waveguide-cavity system with respect to the positions of the rods. In Fig. 5, we compare the original transmission spectrum (the blue curve) with the transmission spectra when the 3rd rod is moved forward and backward in the horizontal direction by the distance $p_3 = 0.01L$. For these two cases, the complex resonant frequencies are $\omega L/(2\pi c) = 0.3794832 - 0.0000424i$ and $\omega L/(2\pi c) =$

$n_{1,3} - n_1$	Taylor I	Exact value
0.03	0.3786297-0.0000411i	0.3786305-0.0000411i
0.09	0.3781368-0.0000398i	0.3781435-0.0000399i
0.15	0.3776439-0.0000385i	0.3776600-0.0000389i
-0.03	0.3791226-0.0000424i	0.3791235-0.0000424i
-0.09	0.3796155-0.0000436i	0.3796247-0.0000438i
-0.15	0.3801084-0.0000449i	0.3801365-0.0000454i

Table 6. Excat and approximates values of the normalized resonant frequency, $\omega L/(2\pi c)$, for a few values of $n_{1,3}$.
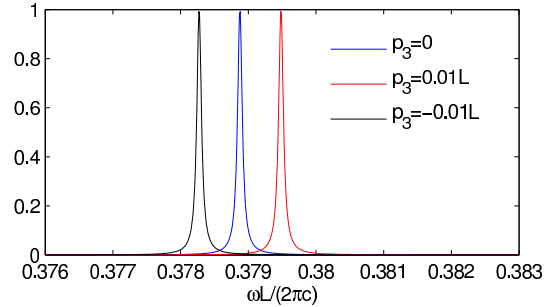
Fig. 5. Transmission spectra of the waveguide-cavity system shown in Fig. 3 (blue curve) and perturbed systems with rod 3 moved in the horizontal direction by $0.01L$ (red curve) and $-0.01L$ (black curve).

$0.3782736 - 0.0000410i$, respectively. These results are obtained using the DtN-map method summaried in Section 3. Notice that the real parts of the complex resonant frequencies correspond exactly to the frequencies of the transmission peaks in the spectra.

Using the method of Section 5, we calculate the partial derivatives of the complex resonant frequency with respect to the positions of the eight rods shown in Fig. 3. Table 7 lists

Rod no. i	v_i	$L^2/(2\pi c)\,\partial\omega/\partial p_i$
1	(1,0)	0.0004634-0.0000427i
2	(1,0)	0.0040980-0.0000092i
3	(1,0)	0.0604804-0.0000711i
7	(0,-1)	0.0604966-0.0000185i

Table 7. Partial derivatives of the complex resonant frequency ω with respect to the moving distances in horizontal or vertical directions of selected rods.

$\partial\omega/\partial p_i$ for four rods moving horizontally or vertically towards the center of the microcavity (if $p_i > 0$). More precisely, we choose $v_i = (1,0)$ for rods 1, 2 and 3, and $v_7 = (0,-1)$ for rod 7. These partial derivatives are evaluated at $p_i = 0$. Since the real and imaginary parts of $\partial\omega/\partial p_i$ are positive and negative, respectively, as a rod is moved toward the center, the real resonant frequency will increase, the transmission peak will blueshift, the imaginary part of ω (which is originally nagative) will have a larger magnitude, and the Q factor of the resonant mode will decrease. It is also clear that the resonant frequency is more

sentitive to the two rods (3 and 7) that are closer to the center. Due to the reflection symmetries in both x and y directions, the partial derivatives for rods 4, 5, 6 and 8 are exactly the same as those for rods 3, 2, 1 and 7, if we choose $v_i = (-1, 0)$ for rods 4, 5, 6, and $v_8 = (0, 1)$ for rod 8.

The first order derivatives allow us to estimate the complex resonant frequency when a rod is moved by a small distance. In Table 8, we compare the exact and approximate values of ω

p_3/L	Taylor I	Exact value
0.002	0.3789971−0.0000419i	0.3789972−0.0000419i
0.004	0.3791181−0.0000420i	0.3791184−0.0000420i
0.006	0.3792390−0.0000421i	0.3792398−0.0000421i
0.008	0.3793600−0.0000423i	0.3793614−0.0000423i
0.010	0.3794809−0.0000424i	0.3794832−0.0000424i
−0.002	0.3787552−0.0000416i	0.3787553−0.0000416i
−0.004	0.3786342−0.0000414i	0.3786346−0.0000414i
−0.006	0.3785133−0.0000413i	0.3785141−0.0000413i
−0.008	0.3783923−0.0000411i	0.3783938−0.0000412i
−0.010	0.3782713−0.0000410i	0.3782736−0.0000410i

Table 8. Exact and approximate values of the normalized resonant frequency, $\omega L/(2\pi c)$, for a few values of p_3 with fixed $v_3 = (1, 0)$.

when rod 3 is moved slightly in the horizontal direction. The approximate values are obtained by the first order Taylor expansion, and they appear to be quite accurate.

The numerical results of this section are obtained using $N = 13$ points on each edge of the unit cells, and they are validated by additional calculations with even larger N.

7. CONCLUSION

In the previous sections, an efficient method is developed to compute the partial derivatives with respect to geometric and physical parameters for complex frequencies of resonant modes in PhC microcavities. The method is specially designed for idealized 2D photonic crystal devices with circular cylinders (dielectric rods or air-holes), and the relevant parameters are the radii, refractive indices and positions of the cylinders. The method relies on the so-called DtN-map method for PhC devices [10, 13] to take advantage of the identical unit cells and the analytic solutions for circular cylindrical structures, and to solve the problems in very small truncated domains. In particular, our method is capable of rapidly computing the partial derivatives with respect to the parameters of many different unit cells. To simplify the presentation, we concentrate on simple microcavities in a PhC with a square lattice of dielectric rods for the E polarization, but the method is applicable to more complicated structures and to the H polarization, including those in PhCs with a triangular lattice of air-holes [16].

Practical PhC microcavities are often fabricated on PhC slabs. Unfortunately, the DtN-map method has only limited success for analyzing three-dimensional devices on PhC slabs [17–19]. An important reason is that the rigorous boundary conditions for terminating the PhC waveguides, i.e., Eqs. (5) and (6), are too expensive to construct for 3D structures. However, in the

case when the out-of-plane radiation loss is small, 2D models for PhC slab devices can capture some physics at least qualitatively, and our method may be used to gain a basic understanding about the sensitivity of resonant modes in PhC slab structures. Another limitation of our method is the requirement for circular cylinders in the PhC devices, since we used analytic solutions to construct the DtN maps of the unit cells and to calculate their derivatives. It is clearly important to develop a more general method so that the effect of noncircular deformations to cylinders in PhC devices can be easily analyzed.

APPENDIX A

For a square unit cell Ω_i given by $|x| < L/2$ and $|y| < L/2$, containing a circular rod given by $r < a$, where r and θ are the polar coordinates and a is the radius of the rod, the DtN map of Ω_i for Eq. (1) is approximated by a $(4N) \times (4N)$ matrix $\Lambda_i = ND^{-1}$, where D and N are related to $4N$ analytic solutions

$$\Phi_l(r) = \phi_m(r)e^{im\theta}, \quad l = 1, 2, ..., 4N, \tag{29}$$

for $m = l - 2N - 1$, and

$$\phi_m(r) = \begin{cases} J_m(k_0 n_1 r), & r < a, \\ A J_m(k_0 n_2 r) + B Y_m(k_0 n_2 r), & r > a. \end{cases} \tag{30}$$

In the above, n_1 and n_2 are the refractive indices of the rod and the medium outside the rod, respectively, coefficients A and B satisfy

$$J_m(k_0 n_2 a)A + Y_m(k_0 n_2 a)B = J_m(k_0 n_1 a), \tag{31}$$
$$J_m'(k_0 n_2 a)A + Y_m'(k_0 n_2 a)B = \rho J_m'(k_0 n_1 a), \tag{32}$$

where $\rho = n_1/n_2$ for the E polarization and $\rho = n_2/n_1$ for the H polarization, J_m and Y_m are Bessel functions, J_m' and Y_m' are their derivatives. The entries of D and N are simply $\Phi_l(r)$ and $v(r) \cdot \nabla \Phi_l(r)$, evaluated at $4N$ points on the boundary of Ω_i and $v(r)$ is a unit normal vector of the boundary [11, 12].

If the center of the rod is shifted to $p_i v_i$, where v_i is a fixed unit vector, then we need to replace $\Phi_l(r)$ by $\Phi_l(r - p_i v_i)$ in the construction of the DtN map. Notice that

$$\frac{\partial \Phi_l}{\partial p_i}(r - p_i v_i)\Big|_{p_i=0} = -(v_i \cdot \nabla)\Phi_l(r),$$

$$\frac{\partial \nabla \Phi_l}{\partial p_i}(r - p_i v_i)\Big|_{p_i=0} = -(v_i \cdot \nabla)\nabla \Phi_l(r),$$

$$\frac{\partial^2 \Phi_l}{\partial p_i^2}(r - p_i v_i)\Big|_{p_i=0} = (v_i \cdot \nabla)^2 \Phi_l(r),$$

$$\frac{\partial^2 \nabla \Phi_i}{\partial p_i^2}(r - p_i v_i)\Big|_{p_i=0} = (v_i \cdot \nabla)^2 \nabla \phi_l(r).$$

Therefore, to evaluate the first and second order derivatives of D and N, we need the partial derivatives of Φ_l up to the third order.

The gradient of Φ_l is

$$\nabla \Phi_l = \left[\phi_m' \begin{pmatrix} \cos\theta \\ \sin\theta \end{pmatrix} + \frac{im\phi_m}{r} \begin{pmatrix} -\sin\theta \\ \cos\theta \end{pmatrix} \right] e^{im\theta},$$

where ϕ'_m is the derivative of ϕ_m with respect to r. We need to use the expression of ϕ_m for $r > a$, thus the partial derivatives of Φ_l are

$$\frac{\partial \Phi_l}{\partial x}(\boldsymbol{r}) = k_0 n_2 ps - imqt,$$

$$\frac{\partial \Phi_l}{\partial y}(\boldsymbol{r}) = k_0 n_2 pt + imqs,$$

$$\frac{\partial^2 \Phi_l}{\partial x^2}(\boldsymbol{r}) = k_0 n_2 \left(p_1 s + ps_1 \right) - im \left(q_1 t + qt_1 \right),$$

$$\frac{\partial^2 \Phi_l}{\partial y^2}(\boldsymbol{r}) = k_0 n_2 \left(p_2 t + pt_2 \right) + im \left(q_2 s + qs_2 \right),$$

$$\frac{\partial^2 \Phi_l}{\partial x \partial y}(\boldsymbol{r}) = k_0 n_2 \left(p_2 s + ps_2 \right) - im \left(q_2 t + qt_2 \right),$$

$$\frac{\partial^3 \Phi_l}{\partial x^3}(\boldsymbol{r}) = k_0 n_2 \left(p_3 s + 2 p_1 s_1 + ps_3 \right) - im \left(q_3 t + 2 q_1 t_1 + qt_3 \right),$$

$$\frac{\partial^3 \Phi_l}{\partial y^3}(\boldsymbol{r}) = k_0 n_2 \left(p_4 t + 2 p_2 t_2 + pt_4 \right) + im \left(q_4 s + 2 q_2 s_2 + qs_4 \right),$$

$$\frac{\partial^3 \Phi_l}{\partial x^2 \partial y}(\boldsymbol{r}) = k_0 n_2 \left(p_5 s + p_1 s_2 + p_2 s_2 + ps_5 \right)$$
$$- im \left(q_5 t + q_1 t_2 + q_2 t_1 + qt_5 \right),$$

$$\frac{\partial^3 \Phi_l}{\partial x \partial y^2}(\boldsymbol{r}) = k_0 n_2 \left(p_5 t + p_1 t_2 + p_2 t_1 + pt_4 \right)$$
$$+ im \left(q_5 s + q_1 s_2 + q_2 s_1 + qs_5 \right),$$

where

$$p = AJ'_m(k_0 n_2 r) + BY'_m(k_0 n_2 r),$$
$$q = [AJ_m(k_0 n_2 r) + BY_m(k_0 n_2 r)]/r,$$
$$s = e^{im\theta} \cos(\theta),$$
$$t = e^{im\theta} \sin(\theta),$$

and the subscripts 1, 2, 3, 4 and 5 (of p, q, s and t) are used to denote the partial derivatives corresponding to ∂_x, ∂_y, ∂_x^2, ∂_y^2 and ∂_{xy}^2, respectively.

APPENDIX B

The partial derivative of $\boldsymbol{\Lambda}_i$ with respect to ω is related to the corresponding partial derivatives of $\boldsymbol{D}$ and $\boldsymbol{N}$, and they are further related to the partial derivatives of ϕ_m and ϕ'_m with respect to ω. For simplicity, we define the normalized frequency $\hat{\omega} = \omega L/(2\pi c) = k_0 L/(2\pi)$, then

$$\frac{\partial \phi_m}{\partial \hat{\omega}}(r) = \frac{\partial A}{\partial \hat{\omega}} J_m(z) + \frac{\partial B}{\partial \hat{\omega}} Y_m(z) + br[AJ'_m(z) + BY'_m(z)],$$

$$\frac{\partial \phi'_m}{\partial \hat{\omega}}(r) = k_0 n_2 \left[\frac{\partial A}{\partial \hat{\omega}} J'_m(z) + \frac{\partial B}{\partial \hat{\omega}} Y'_m(z) \right]$$
$$+ bA[J'_m(z) + zJ''_m(z)] + bB[Y'_m(z) + zY''_m(z)],$$

where $b = 2\pi n_2/L$ and $z = k_0 n_2 r$. Notice that the coefficients A and B depend on ω. From Eqs. (31) and (32), we obtain

$$A = \frac{\rho s' q - sq'}{C}, \quad B = \frac{sp' - \rho ps'}{C}, \tag{33}$$

where

$$p = J_m(k_0 n_2 a),$$
$$p' = [J_{m-1}(k_0 n_2 a) - J_{m+1}(k_0 n_2 a)]/2,$$
$$p'' = [J_{m-2}(k_0 n_2 a) - 2J_m(k_0 n_2 a) + J_{m+2}(k_0 n_2 a)]/4,$$

q, q' and q'' are defined as above with J_m replaced by Y_m, s, s', s'' are defined with J_m but with n_2 replaced by n_1, and $C = qp' - pq'$. Then,

$$\frac{\partial A}{\partial \hat{\omega}} = \frac{F}{G}, \quad \frac{\partial B}{\partial \hat{\omega}} = \frac{H}{G},$$

where

$$F = abC(\rho^2 s'' - sq'') - ab(\rho s' q - sq')(qp'' - pq''),$$
$$H = abC(sp'' - \rho^2 ps'') - ab(sp' - \rho ps')(qp'' - pq''),$$
$$G = C^2.$$

The partial derivatives with respect to the refractive index n_1 can be similarly evaluated. We have

$$\frac{\partial \phi_m}{\partial n_1}(r) = \frac{\partial A}{\partial n_1} J_m(z) + \frac{\partial B}{\partial n_1} Y_m(z),$$

$$\frac{\partial \phi'_m}{\partial n_1}(r) = k_0 n_2 \left[\frac{\partial A}{\partial n_1} J'_m(z) + \frac{\partial B}{\partial n_1} Y'_m(z) \right],$$

where A and B are given in Eq. (33). Simple calculations lead to

$$\frac{\partial A}{\partial n_1} = \frac{M}{C}, \quad \frac{\partial B}{\partial n_1} = \frac{N}{C}$$

for the E polarization, where C is defined above and

$$M = \frac{1}{n_2} s' q + k_0 a(\rho s'' q - s'q'),$$

$$N = k_0 a(s'p' - \rho ps'') - \frac{1}{n_2} ps'.$$

REFERENCES

1. K. K. Choi, "Shape design sensitivity analysis and optimal design of structural systems," in S. A. Mota Soares (ed.), *Computer Aided Optimal Design: Structural and Mechanical Systems*, Springer-Verlag, Berlin, pp. 439-492 (1987).
2. K. Svanberg, "The method of moving asymptotes – a new method for structural optimization," International Journal for Numerical Methods in Engineering **24**(2), 359-373 (1987).
3. N. K. Georgieva, S. Glavic, M. H. Bakr, and J. W. Bandler, "Feasible adjoint sensitivity technique for EM design optimization," IEEE Trans. Microwave Theory Tech. **50**, 2751-2758 (2002).
4. G. Veronis, R. W. Dutton, and S. Fan, "Method for sensitivity analysis of photonic crystal devices," Opt. Lett. **29**, 2288-2290 (2004).
5. C. M. Lalau-Keraly, S. Bhargava, O. D. Miller, and E. Yablonovitch, "Adjoint shape optimization applied to electromagnetic design," Opt. Express **21**, 21693-21701 (2013).
6. A. C. R. Niederberger, D. A. Fattal, N. R. Gauger, S. Fan, and R. G. Beausoleil, "Sensitivity analysis and optimization of sub-wavelength optical gratings using adjoints," Opt. Express **22**, 12971-12981 (2014).
7. Z. Hu and Y. Y. Lu, "Second order sensitivity analysis for a photonic crystal waveguide bend," J. Opt. Soc. Am. B **32**, 69–75 (2015).
8. J. Smajic, C. Hafner, and D. Erni, "Design and optimization of an achromatic photonic crystal bend," Opt. Express **11**, 1378-1384 (2003).
9. D. Joannopoulos, S. G. Johnson, J. N. Winn, and R. D. Meade, *Photonic Crystals: Molding the Flow of Light,* 2nd ed. (Princeton University Press, Princeton, NJ, 2008).
10. Z. Hu and Y. Y. Lu, "Efficient analysis of photonic crystal devices by Dirichlet-to-Neumann maps," Opt. Express **16**, 17383-17399 (2008).

11. Y. Huang and Y. Y. Lu, "Scattering from periodic arrays of cylinders by Dirichlet-to-Neumann maps," J. Lightw. Technol. **24**, 3448-3453 (2006).

12. J. Yuan and Y. Y. Lu, "Photonic bandgap calculations using Dirichlet-to-Neumann maps," J. Opt. Soc. Am. A **23**, 3217–3222 (2006).

13. S. Li and Y. Y. Lu, "Efficient method for analyzing leaky cavities in two-dimensional photonic crystals," J. Opt. Soc. Am. B **26**, 2427–2433 (2009).

14. Y. Huang, Y. Y. Lu, and S. Li, "Analyzing photonic crystal waveguides by Dirichlet-to-Neumann maps," J. Opt. Soc. Am. B **24**, 2860–2867 (2007).

15. L. N. Trefethen and D. Bau, *Numerical Linear Algebra*, (Society of Industrial and Applied Mathematics, Philadelphia, 1997).

16. Z. Hu and Y. Y. Lu, "Efficient numerical modeling of photonic crystal heterostructure devices," J. Lightw. Technol. **33**(10), 2012–2018 (2015).

17. L. Yuan and Y. Y. Lu, "Dirichlet-to-Neumann map method for analyzing hole arrays in a slab," J. Opt. Soc. Am. B **27**(12), 2568–2579 (2010).

18. L. Yuan and Y. Y. Lu, "An efficient numerical method for analyzing photonic crystal slab waveguides," J. Opt. Soc. Am. B **28**, 2265–2270 (2011).

19. L. Yuan and Y. Y. Lu, "Mode reduction for efficient modeling of photonic crystal slab structures," J. Lightw. Technol. **32**(13), 2340–2344 (2014).